

Supplementary Data for:**Bioactivation of the human carcinogen aristolochic acid**

Viktoriya S. Sidorenko^{1*}, Sivaprasad Attaluri¹, Irina Zaitseva¹, Charles R. Iden¹, Kathleen

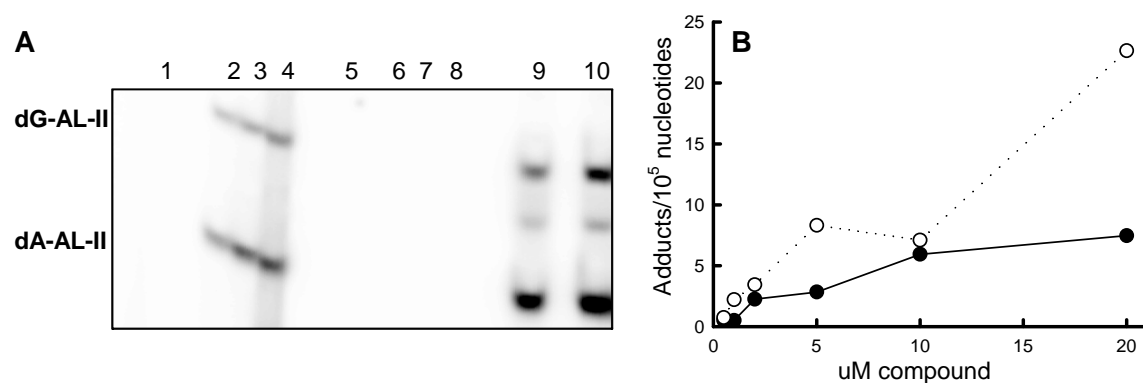
Dickman^{1,2}, Francis Johnson^{1,3}, Arthur P. Grollman^{1,2}

Contents

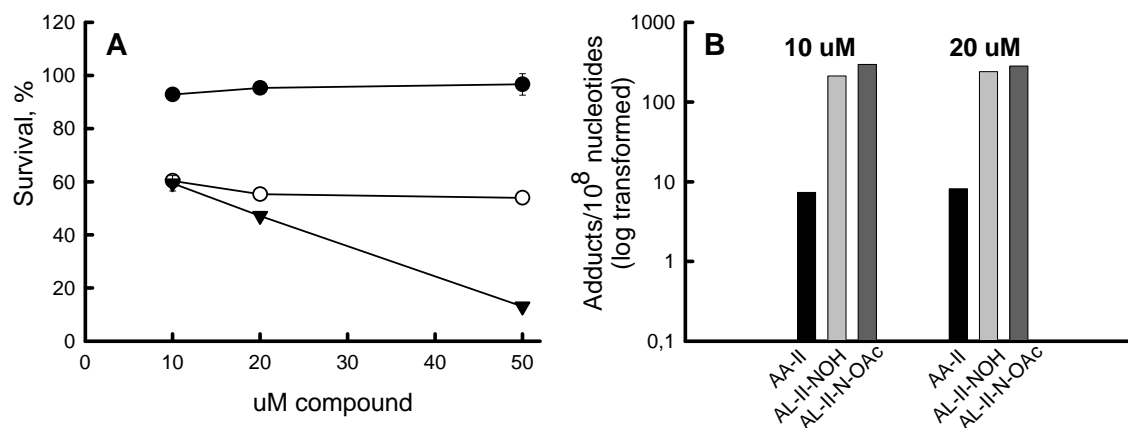
- p2. Supplementary Table S1. Activation of AL-I-NOH and AL-II-NOH by human SULTs.
- p3. Supplementary Figure S1. Reactivity of AA-II and its analogs with DNA.
- p4. Supplementary Figure S2. Cytotoxicity and genotoxicity of AA-II and its analogs in human fibroblasts cell line.
- p5. Figure S3. Stability of AA-I metabolites.
- p6. Supplementary Figure S4. SULT1A activation of AL-I-NOH and AL-II-NOH.
- p7. Supplementary Figure S5. NAT2 activation of AL-I-NOH.
- p8. Supplementary Figure S6. SULT1B1 stimulates AA-II activity in the presence of NQO1.
- p9. Supplementary Figure S7. Full size polyacrylamide gels.

Supplementary Table S1. Activation of AL-I-NOH and AL-II-NOH by human SULTs. DNA was incubated for 1-6 hr with AL-I-NOH or AL-II-NOH and PAPS in the presence of 10-40 nM of SULT1 enzymes. Initial rates of AL-DNA adduct formations were calculated as described for SULT1B1 (see **Fig. 4** and **Supplementary Fig. 4**). Initial rates are presented as a fraction of the initial rate of SULT1B1 for 10, 20 and 40 nM enzyme, and correspond to 20.4, 30.4 and 50.9 AL-I-DNA adducts/ 10^6 nucleotides/h and 3.1, 8.7 and 26.6 AL-II-DNA adducts/ 10^6 nucleotides/h, respectively. Mean values across all doses and standard deviations for three independent experiments are shown.

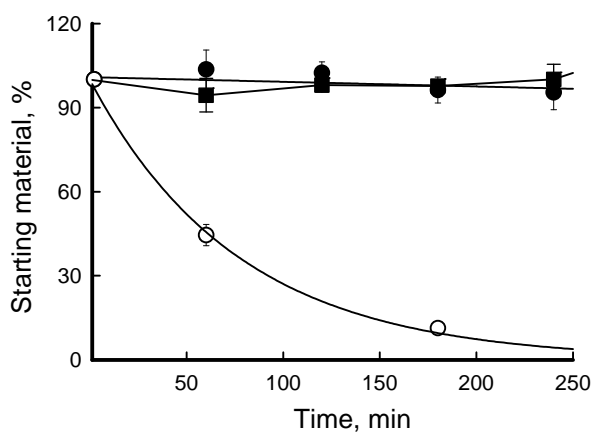
Enzyme	Adduct analysis activity % of SULT1B1 initial rate	
	AL-I-DNA	AL-II-DNA
SULT1B1	100.0 ± 11.8	100.0 ± 4.9
SULT1A1	2.8 ± 1.0	68.0 ± 4.0
SULT1A2	6.0 ± 2.7	44.8 ± 3.3
SULT1A3	0.2 ± 0.1	78.9 ± 12.9



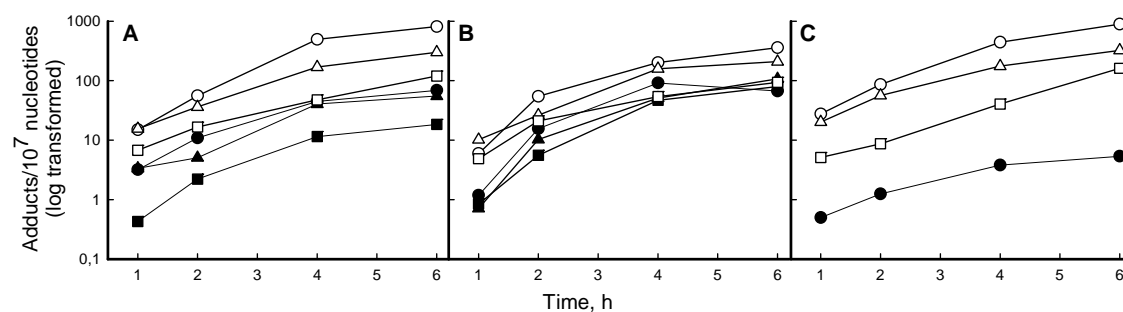
Supplementary Figure S1. Reactivity of AA-II and its analogs with DNA. AA-II, AL-II-NOH and AL-II-N-OAc were incubated with DNA in the presence and absence of zinc powder, 2 mg per reaction, and analyzed for adducts as described in Materials and Methods. **(A)** The fragment of a 30% polyacrylamide gel after ³²P-labeling of DNA adduct nucleosides. dG-AL-II or dA-AL-II, the upper and lower band respectively. The middle band is the product of incomplete digestion. 1 – 20 uM AA-II and DNA, incubation for 4 h without zinc; 2-4 – incubations of AA-II, DNA and zinc for 1, 2, 4 h, respectively; 5 – AL-II-NOH and DNA incubation for 4 h without zinc; 6-8 – AL-II-NOH, DNA and zinc incubations for 1, 2, 4 h, respectively; 9-10 – 20 uM AL-II-N-OAc, DNA 4 h incubations in the presence and absence of zinc, respectively. **(B)** Dose dependent AL-II-DNA adducts formation. DNA, AA-II or AL-II-N-OAc was incubated for 2 h with or without zinc, respectively. DNA was subjected to adduct analysis. Filled circles (●) indicate AL-II-DNA adducts in the presence AA-II and zinc, open circles (○) – AL-II-DNA adducts in the presence of AL-II-N-OAc and the absence of zinc. Each point corresponds to mean values for at least two independent experiments.



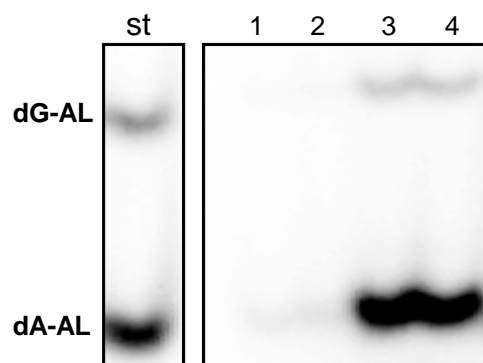
Supplementary Figure S2. Cytotoxicity and genotoxicity of AA-II and its analogs in human fibroblasts cell line. The GM00637 human fibroblast cell line was treated with various aristolatum II analogs at the concentrations shown for 48 h and 24 h, then analyzed for cytotoxicity and genotoxicity, respectively. **(A)** Cytotoxicity as measured by ATP assay in human fibroblasts treated with; (●) filled circles AA-II, (○) open circles AL-II-NOH; (▼) filled triangles AL-II-N-OAc. **(B)** AL-II-DNA adducts in cells treated with 10 and 20 uM of the compounds. Results are shown as mean values for two independent experiments.



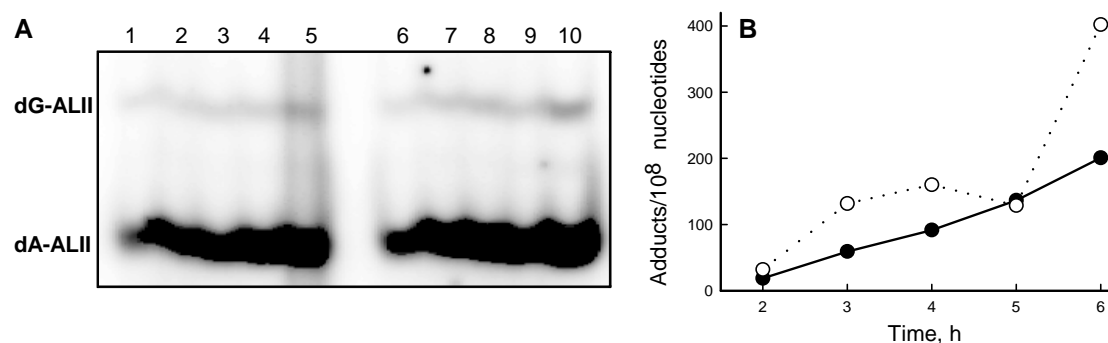
Supplementary Figure S3. Stability of AA-I metabolites. Decomposition of AL-I-NOH (●) filled circles, AL-I-N-OSO₃H (○) open circles and AL-I-N-OAc (■) filled squares was monitored over time by HPLC. Peak areas detected by UV absorption at 254 nm were used to determine the stability of each compound. Results are shown as mean values and standard deviations for three independent experiments.



Supplementary Figure S4. SULT1A activation of AL-I-NOH and AL-II-NOH. Calf thymus DNA was incubated for 1-6 h with 100 μ M of AL-I-NOH (filled symbols) or AL-II-NOH (open symbols) and 80 (circles), 40 (triangles), and 10 nM (squares) SULT1A enzymes in the presence of PAPS. DNA (2-5 μ g) was used for the adduct analysis. **(A)** Shows time dependence of AL-I- and AL-II-DNA adducts formation in the presence of SULT1A1. **(B and C)** The same for SULT1A2 and SULT1A3, respectively. Results are shown as mean values for three independent experiments. Initial rates for each dose of enzyme were calculated using linear regression analysis in Sigma Plot and shown as percentage from SULT1B1 activity across all doses in **Supplementary Table 1**.

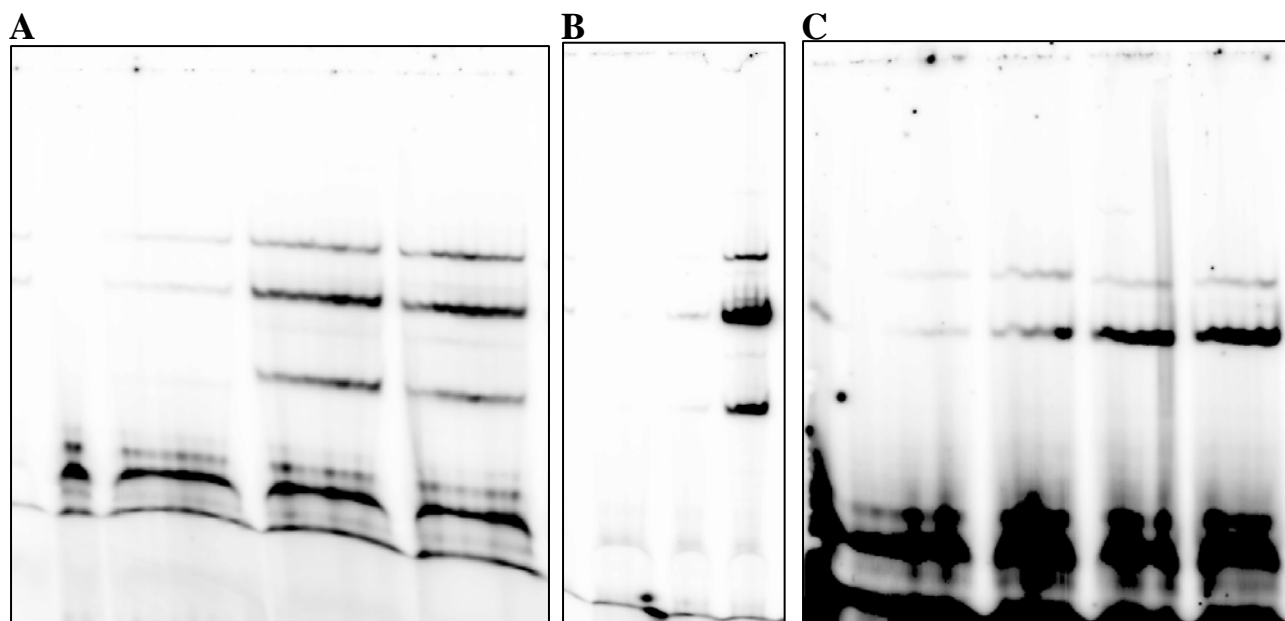


Supplementary Figure S5. NAT2 activation of AL-I-NOH. Salmon sperm DNA was incubated with 100 μ M of AL-I-NOH in the presence of acetyl-CoA and NAT1 or NAT2 for 4 and 6 h. After reaction DNA was analyzed for AL-I-DNA adduct presence by 32 P-postlabeling. The fragment of a 30% polyacrylamide gel is shown. St – Mixture of 24-mer oligonucleotides (60 fmol) containing a single dG-AL-II or dA-AL-II, represented by the upper and lower band, respectively. Lanes 1-2 – incubations of DNA with AL-I-NOH, acetyl-CoA and NAT1 for 4 and 6 h, respectively; 3-4 – the same for NAT2.



Supplementary Figure S6. SULT1B1 stimulates AA-II activity in the presence of NQO1.

AA-II, 100 μ M, was incubated with DNA, PAPS, NADPH, 500 nM of each, SULT1B1 and/or NQO1. 20 μ g of DNA was used for the adduct analysis. **(A)** The fragment of a 30% polyacrylamide gel after 32 P-labeling of DNA adduct nucleosides. dG-AL-II or dA-AL-II, the upper and lower band respectively. 1-5 – 2, 3, 4, 5, 6 h incubations of AA-II, NQO1 and DNA, respectively; 6-10 – the same for AA-II, NQO1 and SULT1B1. **(B)** Time dependence of AL-II-DNA adducts formation. Filled circles (●) – DNA adducts in the presence of NQO1, open circles (○) – DNA adducts in the presence of SULT1B1 and NQO1. Results are shown as mean values for two independent experiments.



Supplementary Figure S7. Full size polyacrylamide gels. (A) and (B) represent the full size polyacrylamide gels for **Figure 2** and **Figure 3**, respectively. (C) shows the full size polyacrylamide gel for **Figure 6** and **Supplementary Figure S6**. Due to the high reactivity of the compounds the two bands below dA-AL adduct most likely correspond to aristolactam adducted pyrimidines. The rest of the bands represent unspecific labeled nucleosides and unincorporated labeling material. Experimental details are described in **Materials and Methods** and **Results** sections of the manuscript.